Exploration of the Laser-Assisted Clustering and Reactivity of Trimethylaluminum with and without NH_3

Alexander Demchuk, Steven Simpson, and Brent Koplitz*

Department of Chemistry, Tulane University, New Orleans, Louisiana 70118

Received: October 17, 2002; In Final Form: January 7, 2003

This paper provides results concerning the clustering and laser-assisted reactivity in constrained pulsed gas expansions of trimethylaluminum (TMAl) with and without ammonia. In these experiments, TMAl is introduced with just an Ar buffer gas or co-expanded with ammonia into a high vacuum chamber through a dual-source pulsed nozzle assembly. Independent control of individual gas backing pressures is maintained, and the nozzle assembly can be cooled as well. The output of an ArF excimer laser (193 nm) is focused into the mixing and reaction region of the nozzle source, and a quadrupole mass spectrometer (QMS) is used to characterize the expansion products. Both pressure and laser power dependence studies are used to reveal the origins of individual mass spectral features. Under certain conditions, laser irradiation or expanding, neat TMAl results in the formation of $(CH_3)_{4-x}H_{2-y}Al_2$, where $x = 0, 1$ and $y = 0, 1$. During TMAl expansion with NH_3, the parent ion signal for the Lewis acid−base adduct $(CH_3)_3Al{:}NH_3$ is observed in the gas phase by the QMS. Laser photolysis of the TMAl/NH_3 gas mixture produces reactions involving both precursor and adduct molecules. Also, the formation of a new $(CH_3)_3AlNH_2$ product as a result of NH_2 radical reactivity with the $(CH_3)_3Al{:}NH_3$ adduct, i.e., $(CH_3)_3Al{:}NH_3 + NH_2 \rightarrow (CH_3)_3AlNH_2 + NH_3$, is revealed. Diverse higher mass clusters with Al−N bonded nuclei, e.g., $(CH_3)_kAl_l(NH_2)_m(NH)_n$, have also been observed. Finally, a comparison of aluminum and gallium metal organic species reveals similar propensities for intermolecular association for the two metals.

I. Introduction

In recent years, the field of III−V nitride semiconductor growth, in particular GaN and AlN because of their widespread optoelectronic applications, has expanded at a rapid pace.[1,2] Various techniques have been reported for growing III−V nitride films. Among these techniques, metal organic chemical vapor deposition (MOCVD) is a widely used growth method. The MOCVD process for the growth of III−V materials is typically accomplished by the reaction of metal alkyls with hydrides of the nonmetal components.[1,2] In GaN and AlN growth, trimethylgallium (TMGa) and trimethylaluminum (TMAl), respectively, are often used as precursors. Unfortunately, MOCVD usually requires a high growth temperature that can be a disadvantage for certain thin film technologies.[3] As an alternative, lasers can be used to facilitate the deposition of compound semiconductors at reduced temperatures.[4−6]

At the heart of the MOCVD field lies a rich but complicated chemistry. Important molecular questions remain regarding the reactivity of gas−gas, gas−surface, and surface−surface species in growth environments, particularly for materials such as AlN or GaN.[1,2] Although laser-assisted film growth has been previously studied in our laboratory,[7] it is not the primary subject of this paper. Rather, in the current work an excimer laser is used to initiate chemistry in a clustering, reactive environment. As a means of exploring the early stages of gas-phase reactivity, a pulsed laser is useful as a way to deliver photons to activate a metal alkyl/ammonia mixture. Chemically, it is thought that the main gas-phase reaction at low temperatures in these systems is directed by strong Lewis acid−base interactions between the metal alkyl (electron acceptor) and ammonia (electron donor) to form the Lewis acid−base adduct $(CH_3)_3M{:}NH_3$, where M is either Al or Ga.[8−11] This adduct is unstable except at low temperature. With heating (>100 °C), the thermal decomposition of the $(CH_3)_3M{:}NH_3$ adduct results in the evolution of methane: $(CH_3)_3M{:}NH_3 \rightarrow (CH_3)_2M{:}NH_2 + CH_4$, and subsequent oligomerization of these species can occur; e.g., $[(CH_3)_2M{:}NH_2]_3$ can be found.[11,12] These so-called "parasitic" reactions have been troublesome in high-temperature MOCVD growth processes of III−V materials.[11] However, this ability to form adducts with III−V "ready" bonds during the mixing of group III and group V precursors may prove useful in the development of low-temperature deposition techniques for III−V compounds.

Previously, we have reported on our efforts to explore low-temperature GaN materials chemistry in a gaseous environment by combining laser photolysis and metal organic molecular beam techniques.[13,14] In this method, a metal organic precursor (trimethyl or triethylgallium) and an ammonia precursor are introduced independently in a high vacuum chamber through a customized dual-source pulsed nozzle assembly. Here, the excimer laser output is focused into the mixing/reaction region of the nozzle source to initiate chemical reactivity in the gas phase. These investigations revealed that extensive formation of GaN-containing species was occurring following irradiation of the precursors with 193 nm light. Subsequently, calculations by Tomoshkin et al. have pointed toward the possible key role that such clusters may play in GaN deposition processes.[15]

In the current paper, we present recent research involving AlN formation in the gas phase initiated by laser photochemical reactions. In particular, we explore the early stages of low-temperature photoassisted gas-phase reactivity and cluster formation in a constrained gas pulse expansion of trimethylaluminum (TMAl) with and without ammonia. Comparisons with gallium metal organic analogues of this system are also

10.1021/jp022252n CCC: $25.00
Published on Web 02/21/2003

discussed. Note that the underlying motivation for the studies is 2-fold. In general, we look for fundamental insight that will aid in understanding general III−V growth processes. However, ways to facilitate and enhance the *laser-assisted* growth of actual AlN films are also sought.

II. Experimental Section

Described previously, the experimental apparatus consists of a high vacuum chamber (base pressure $\sim 10^{-7}$ Torr) containing a quadrupole mass spectrometer (QMS) and a specialized dual pulsed nozzle source.[13,14] The TMAl (98% minimum purity; Strem Chemical) and the ammonia gas (99.99% purity; Air Products) are introduced into the high vacuum chamber via a nozzle assembly. For the TMAl, an Ar carrier gas (99.9995% purity; Nova Gas) is used. The vapor of the TMAl is introduced into the sample chamber by passing the Ar carrier gas through a temperature-controlled stainless steel bubbler. In the experiments reported here, the NH_3 backing pressure was typically ~2200 Torr, whereas the TMAl sample pressure was usually ~100 Torr in ~3700 Torr of carrier gas. The individual backing pressures, however, were varied from 100 to 4000 Torr as needed to examine pressure effects during certain experiments. Procedurally, a pulse of each sample gas is simultaneously injected into the mixing/reaction region of the nozzle assembly, which can be cooled to 0 °C. From point of mixing, the gases travel through a nozzle extender thereby creating a constrained expansion. The opening time of each pulsed valve was adjusted from ~0.2 to 0.4 ms with repetition rates of 10 Hz. In some experiments, ND_3 (99% D-atom purity; Cambridge Isotope Lab) was used to help identify products and trace reaction pathways.

To initiate photochemistry, the 193 nm output from an ArF excimer laser (Lambda Physik LEXtra 200) is focused into the mixing/reaction region of the nozzle through a 0.7 mm diameter aperture. Laser beam pulse energies ranging from 0.1 to 20 mJ/pulse were used. The focusing lens has a focal length of 250 mm. The delay time between gas sample injection and laser pulse (typically ~5 ms) was adjusted to maximize product signal. The reaction products formed within the nozzle/reaction zone are mass analyzed by an Extrel MEXM2000 quadrupole mass spectrometer (QMS) with a cross beam electron impact (EI) deflector ionizer. For illustration, a depiction of the interaction and detection region is shown in Figure 1. To minimize fragmentation of the reaction products, the electron energy of the ionizer was fixed at 30 eV for all experiments.

III. Results and Discussion

With TMAl as the metal organic target species, experiments were undertaken with and without laser initiation as well as with and without NH_3. The following results are organized according to the conditions under which the experiments were performed. Note that in many of the figures presented, the results are displayed in subtraction mode. Typically in these cases, the signal recorded when no laser beam is present is subtracted from the signal observed when the laser beam is present. Positive features correlate with reactivity induced by the laser, whereas negative peaks correspond to signals that are diminished due to the action of the laser. Subtraction spectra are also presented for binary mixtures. In this case, the contribution due solely to one of the reacting species is subtracted.

A. TMAl Expansion without Laser Radiation. In the absence of laser radiation, the TMAl gas expansion conditions (e.g., gas pressure and nozzle temperature) have a large effect on the expansion products. Parts a and b of Figure 2 show the higher mass region of the EI mass spectrum for neat TMAl

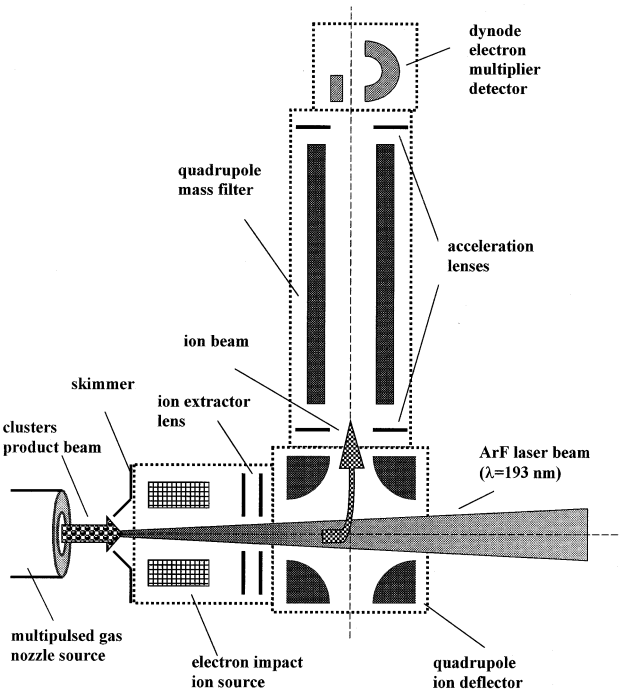

Figure 1. Schematic diagram of the experimental setup for in situ QMS detection of laser-assisted gas-phase reactivity from a nozzle source.

observed under room-temperature nozzle conditions and 0 °C nozzle conditions, respectively. Clearly, cooling the nozzle induces clustering effects, presumably increasing the formation of $[(CH_3)_3Al]_2$, as evidenced by the significant increase in the $Al_2(CH_3)_5^+$ feature as well as other daughter fragments deriving from the TMAl dimer. As expected for dimerization with a nozzle expansion, the intensity of this $Al_2(CH_3)_5^+$ ion signal is strongly dependent on the nozzle temperature. Note that with this experimental setup we have not seen any clustering involving carrier molecules such as Ar or He. In general, we have seen similar behavior regarding TMAl dimer formation if He is used as a carrier, although the influence of Ar carrier gas on TMAl dimer formation is more pronounced as a result of more efficient collisional cooling in the constrained nozzle expansion.

Experimentally, the relative intensity of the $Al_2(CH_3)_5^+$ signal at a given temperature also increases sharply with backing pressure (see Figure 3). This behavior is expected, because it is known that the monomer/dimer ratio depends strongly on the pressure as well as the temperature.[16] Figure 4 illustrates the calculated pressure dependence for the TMAl dimer concentration for the temperatures of 273 and 300 K under equilibrium conditions at a variety of pressures. The curves were calculated using the equilibrium constant given in ref 16. For illustration purposes, 10^{-4} Torr has been indicated in Figure 4 to show how certain pressure−temperature conditions can have a dramatic effect on the generated dimer concentration. Note, however, that the experimental conditions are likely to be far from equilibrium, thus it is difficult to ascertain the pressure and temperature gradients across the constrained expansion. Nonetheless, the significant increase in dimer formation in Figure 2 arising from cooling the nozzle extender suggests that rapid thermal energy exchange between the gas molecules and the extender walls is occurring. Furthermore, by cooling the nozzle assembly, it is now possible to investigate influences of the dimer/monomer ratio on gas-phase reactivity and clustering, as discussed below.

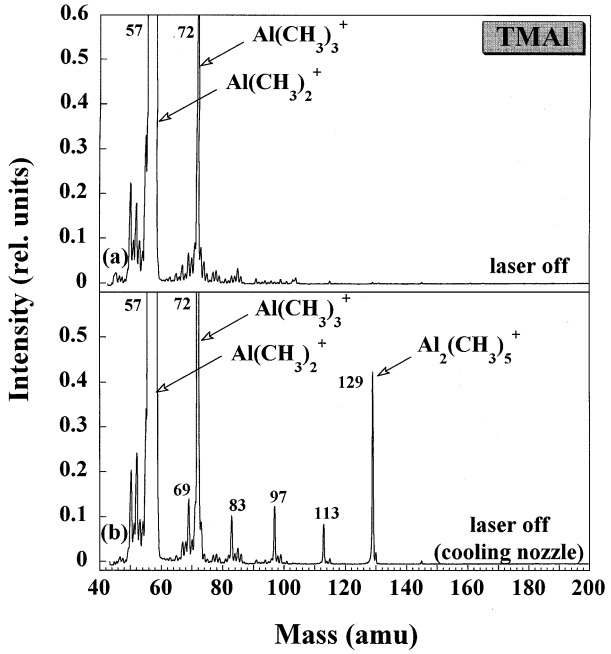

Figure 2. Mass spectra of TMAl expansion (a) without nozzle cooling and (b) when the nozzle is cooled to 0 °C with no laser excitation.

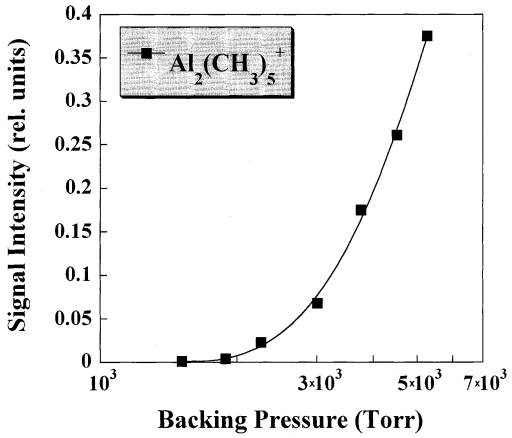

Figure 3. Intensity of ion mass 129 amu, $(CH_3)_5Al_2^+$, as a function of TMAl sample pressure.

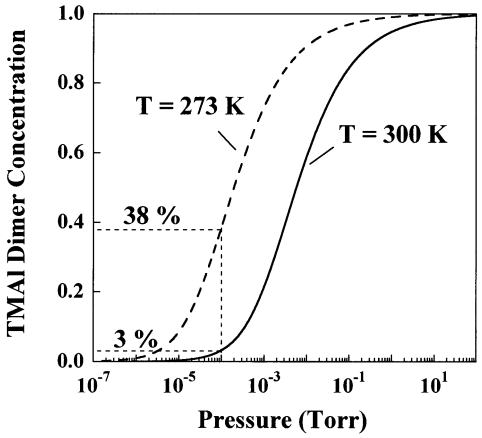

Figure 4. Equilibrium pressure dependence of the TMAl dimer concentration for temperatures of 273 and 300 K. The curves were calculated using the equilibrium constant given in ref 16.

B. Laser-Initiated TMAl Reactivity. Laser irradiation of the expanding TMAl results in the appearance of $Al_2H_{2-y}(CH_3)_{4-x}$ features independent of whether nozzle cooling is used, as is illustrated in Figure 5. Note that the spectra presented in Figure 5b,c were generated by subtracting the associated mass spectrum measured in the absence of laser radiation from the laser-initiated spectrum. Clearly, laser photolysis causes the $Al(CH_3)_3^+$ and $Al_2(CH_3)_5^+$ ion signals to decrease in intensity, as shown by the negative peaks found in Figure 5b,c. Positive peaks show product formation. The dominant new feature is mass 115 that can be attributed to $Al_2H_{2-y}(CH_3)_{4-x}$ formation.

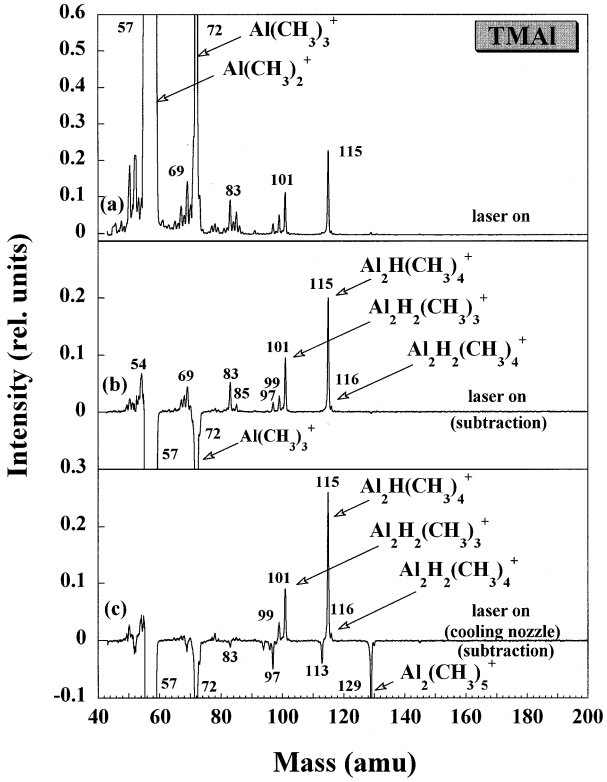

Figure 5. Mass spectra of a TMAl expansion using laser excitation (193 nm, 10 mJ/pulse). For (a) and (b), no nozzle cooling was used. For (c), the nozzle was cooled to 0 °C. In (b) and (c), the reported spectra were obtained after subtracting the signal taken in the absence of laser radiation.

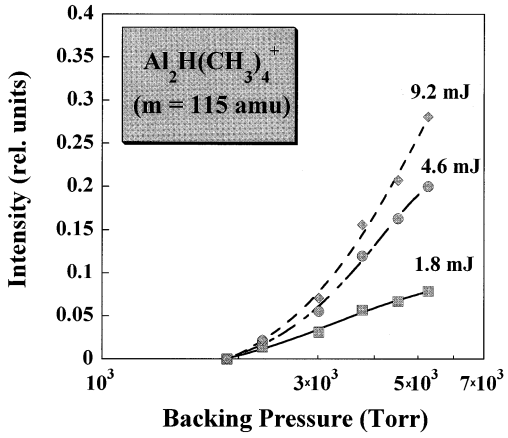

Figure 6. Intensity of ion mass 115 amu as a function of laser intensity.

Mechanistically, the appearance of a dimeric photoproduct is not surprising. It is accepted that the 193 nm photolysis of TMAl can result in a successive release of methyl groups to produce $(CH_3)_{3-x}Al$ species, either through one or multiple photon absorption steps.[17−22] There is also evidence suggesting that a minor channel at higher laser powers is the ejection of a CH_2 group to produce $(CH_3)_2HAl$ via an α-hydrogen elimination route.[17] Though by no means conclusive, the significant presence

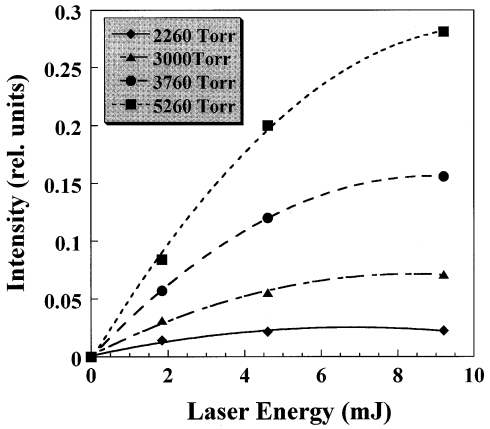

Figure 7. Intensity of ion mass 115 amu as a function of TMAl sample pressure.

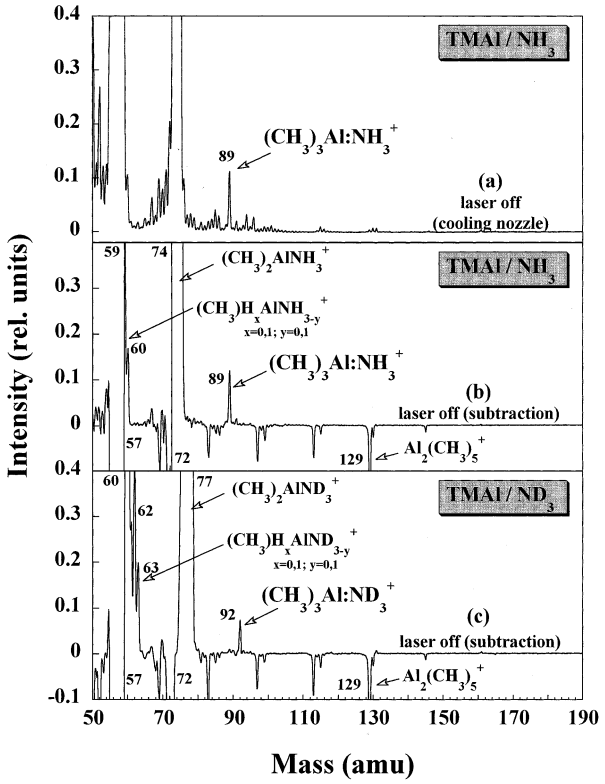

Figure 8. Mass spectra of TMAl/ammonia mixtures in the absence of laser irradiation. In (b) and (c), the reported data were obtained after subtracting the signal taken in the absence of NH_3 and ND_3, respectively. In all cases, the nozzle is cooled to 0 °C.

of the $Al_2H(CH_3)_4^+$ (mass 115) signal along with a small amount of $Al_2H_2(CH_3)_4^+$ (mass 116) is consistent with the $(CH_3)_2HAl$ species playing a role in the observed chemistry, most likely through a photoinitiated reaction to form a bridged species.

Note that the strong $Al_2H(CH_3)_4^+$ ion signal is observed independent of nozzle cooling; in other words it is independent of the TMAl monomer/dimer ratio (see Figure 4). However, its intensity is strongly dependent on the sample gas pressure (Figure 6) similar to what is observed in the TMAl dimer ion signal (Figure 3). Its dependence on laser power (Figure 7) reveals typical saturation behavior with increasing laser fluence. This observation is in good agreement with the aforementioned dimer formation mechanism involving $(CH_3)_2HAl$ radical photogeneration.

Similar behavior was observed during the 193 nm laser photolysis of a gas expansion containing either neat trimethylgallium (TMGa) or triethylgallium (TEGa).[23] A prominent feature was the $R_4HGa_2^+$ ion signal, where R is CH_3 or C_2H_5. Note that in all cases no higher mass clusters (other than the dimer) have been observed under these experimental conditions.

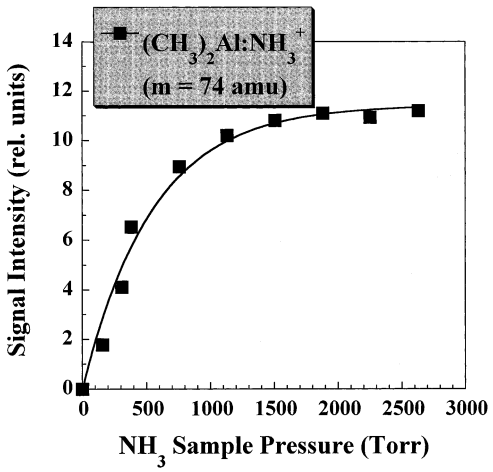

Figure 9. Intensity of ion mass 74 amu, $(CH_3)_2Al:NH_3^+$, in the absence of laser radiation as a function of NH_3 sample pressure. The TMAl sample pressure with Ar carrier gas was equal to 3760 Torr.

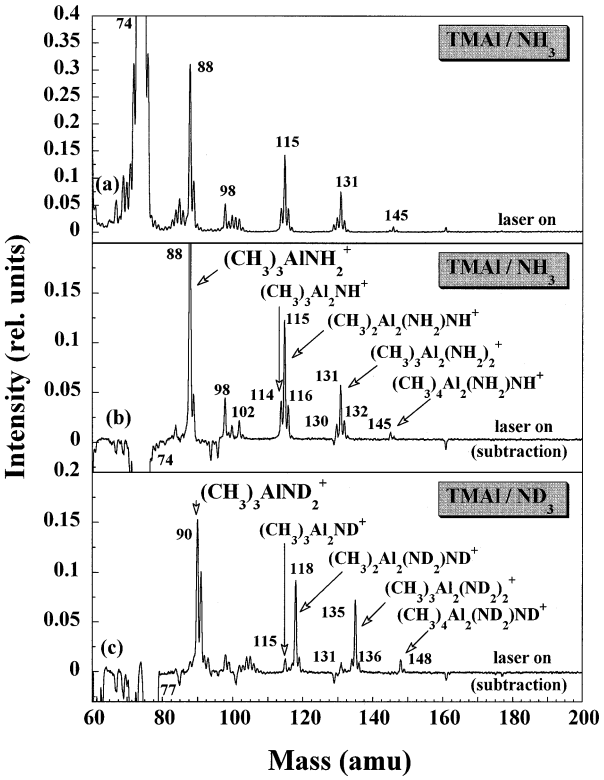

Figure 10. Mass spectra of a TMAl/ammonia expansions using laser excitation (193 nm, 10 mJ/pulse). In (b) and (c), the reported spectra were obtained after subtracting the signal taken in the absence of laser radiation.

C. $TMAl/NH_3$ Reactivity in the Absence of Laser Radiation. When TMAl is expanded with NH_3, the Lewis acid−base adduct formed, $(CH_3)_3Al:NH_3$,[8−11] is readily detected by EI ionization in the gas phase. Figure 8 presents a portion of the higher mass region of the spectra that result when TMAl and NH_3 (or ND_3) are combined in the dual nozzle assembly in the absence of laser radiation. The spectra shown in Figure 8b (TMAl with NH_3) and Figure 8c (TMAl with ND_3) are generated by subtracting an individual TMAl mass spectrum from the spectrum obtained when TMAl and ammonia are mixed. The

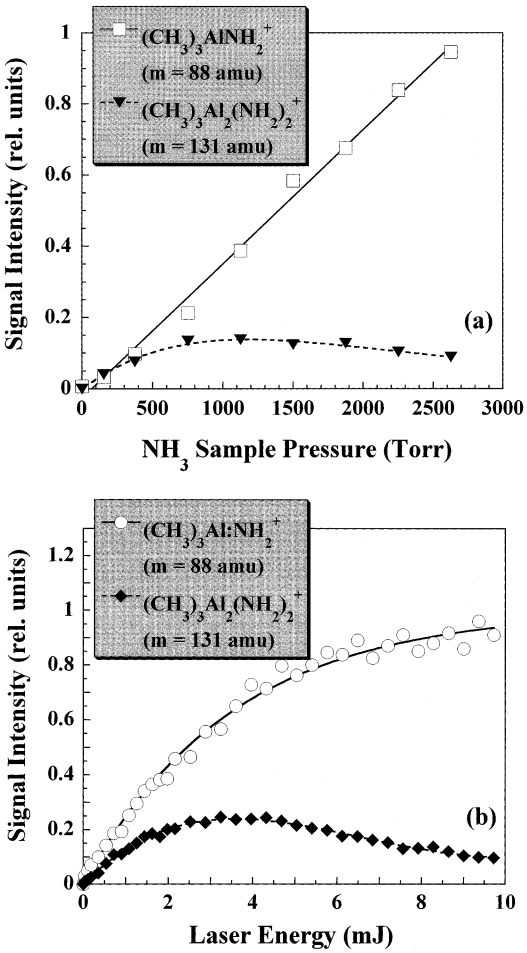

Figure 11. Intensities of ions with mass 88 amu and mass 131 amu as (a) a function of NH_3 sample pressure and (b) as a function of laser pulse energy. The TMAl sample pressure with Ar carrier gas was equal to 3760 Torr.

parent $(CH_3)_3Al{:}NH_3^+$ adduct ion signal at a mass of 89 amu is observed when TMAl and NH_3 are combined under cooled nozzle conditions (Figure 8b), and a strong $(CH_3)_2Al{:}NH_3^+$ daughter ion signal is observed at 74 amu as well. Correspondingly, the $(CH_3)_3Al{:}ND_3^+$ adduct ion signal at mass of 92 amu is detected when ND_3 is used in lieu of NH_3 (Figure 8c), and an associated large ion fragment peak at 77 amu is observed, as expected.

In contrast to the case of TMAl expanding alone, as shown in Figure 2b, it is important to note that under these nozzle cooling conditions there is no significant TMAl dimer signal detected during a TMAl/NH_3 (or ND_3) gas mixture expansion (see Figure 8a). This result suggests that aluminum interacts with the electron donor molecule (NH_3) by breaking Al−C−Al bridges as a result of a strong Al−N interaction,[24]

$$[(CH_3)_3Al]_2 + NH_3 \rightarrow (CH_3)_3Al{:}NH_3 + (CH_3)_3Al \quad (1)$$

thereby producing the observed adduct formation and the disappearance of the dimer.

The intensity of the TMAl:NH_3 adduct signal is greatly dependent on the ammonia pressure. Pressure dependence studies reveal typical saturation behavior for the adduct with increasing ammonia pressure. In Figure 9, a plot of the signal for the TMAl:NH_3 daughter ion, $(CH_3)_2Al{:}NH_3^+$, versus ammonia clearly demonstrates this observation. Note that many of the results presented in the current study were obtained in the TMAl:NH_3 saturation regime, i.e., with an excess of NH_3.

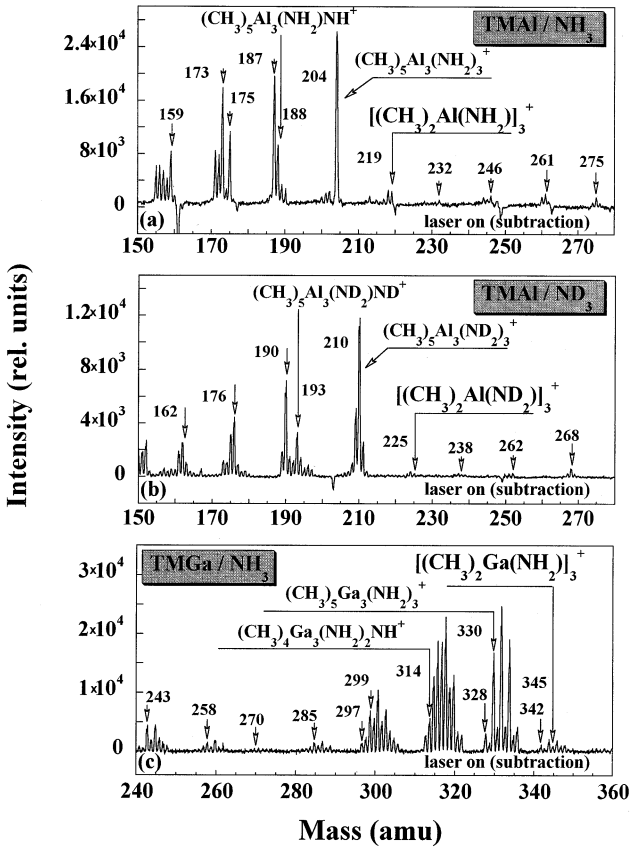

Figure 12. Mass spectra of trimer cluster products generated by the dual gas pulse expansion of (a) TMAl/NH_3, (b) TMAl/ND_3, and (c) TMGa/NH_3 with laser excitation (193 nm, 10 mJ/pulse). The reported spectra were obtained after subtracting the signal taken in the absence of laser radiation.

D. Laser-Initiated TMAl/NH_3 Reactivity. Laser irradiation of an expanding TMAl/NH_3 (or TMAl/ND_3) mixture results in clustering reactions involving precursor and adduct molecules, as illustrated in Figure 10. The spectra shown in Figure 10b,c for reactions involving NH_3 and ND_3, respectively, are displayed in subtraction mode. Laser photolysis causes the adduct intensity to decrease, as evidenced by the negative peaks shown in these spectra. Specifically, the large daughter ion signals at mass 74 (see Figure 10b) and mass 77 (see Figure 10c) are significantly reduced. As shown, a rich spectrum of higher mass products is also generated during laser irradiation of the gas mixtures. These spectra reveal a series of intense higher mass peaks that can be assigned to products containing more than one Al atom such as $(CH_3)_3Al_2(NH_2)_2^+$ and $(CH_3)_2Al_2(NH_2)NH^+$ in the case of NH_3 and the associated deuterated analogues when ND_3 is used. Note that our previous results with trimethylgallium, $(CH_3)_3$-Ga, or triethylgallium, $(C_2H_5)_3Ga$, combined with NH_3 show analogous cluster products.[14]

1. $(CH_3)_3AlNH_2$ Formation. Unambiguously identified in the mass spectrum is the $(CH_3)_3AlNH_2^+$ ion corresponding to mass 88. We call the $(CH_3)_3AlNH_2$ product the "laser-induced adduct" to distinguish it from the $(CH_3)_3Al{:}NH_3$ adduct formed during simple mixing of the gas precursors. This laser-induced adduct displays a linear dependence with increasing ammonia pressure, as shown in Figure 11a. Likewise, the laser power dependence for the $(CH_3)_3AlNH_2^+$ ion signal (see Figure 11b) shows the behavior typical for that of the saturated transition for ammonia irradiated at 193 nm, something that we have observed for the analogous feature in several III−V mixtures.[13,14] Note that the dependence of the $(CH_3)_3AlNH_2$ product on ammonia sample

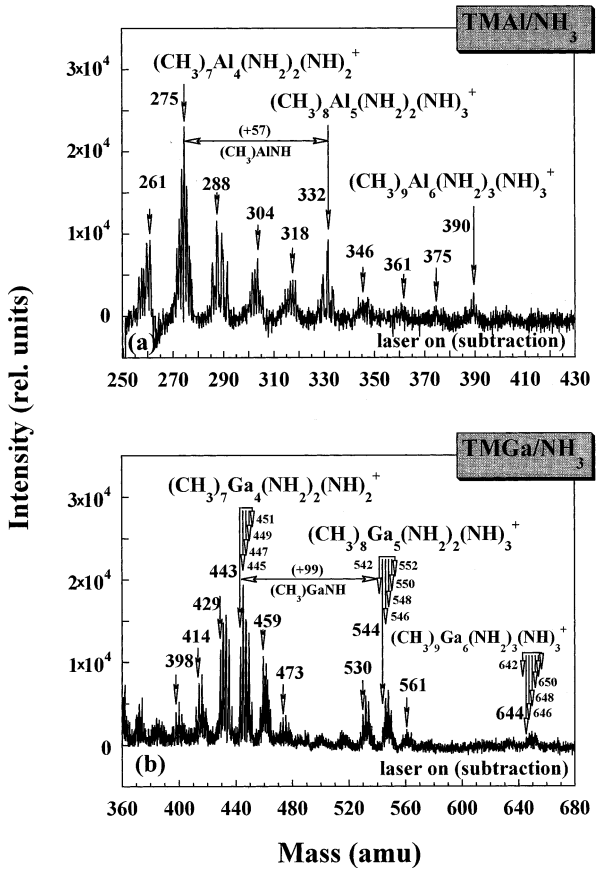

Figure 13. Higher mass cluster products generated by the dual gas pulse expansion of (a) $TMAl/NH_3$ and (b) $TMGa/NH_3$ with laser excitation (193 nm, 10 mJ/pulse). The reported spectra were obtained after subtracting the signal taken in the absence of laser radiation.

pressure and laser power is remarkably different than the behavior observed for higher mass cluster signals, for instance the $(CH_3)_3Al_2(NH_2)_2^+$ feature.

For $(CH_3)_3AlNH_2$, the correlation of the ion signal with NH_3 properties (laser power and pressure) can be attributed to NH_2 radicals undergoing reaction with the $(CH_3)_3Al{:}NH_3$ adduct molecule. The simplest explanation of the source of the $(CH_3)_3AlNH_2$ feature is the photolysis of NH_3 to make NH_2. It is known that NH_3 molecules resonantly absorb 193 nm photons and predissociate on a very short time scale to produce NH_2 radicals with a quantum yield close to unity.[25,26] Subsequent reaction of NH_2 with the $(CH_3)_3Al{:}NH_3$ adduct can form $(CH_3)_3AlNH_2$ and NH_3 in two different ways. Chemically, the simplest route is abstraction of an adduct hydrogen by the NH_2 radical to produce the observed products. This channel is difficult to identify under the current conditions, but experiments using deuterated TMAl (not yet performed) will be useful. Fortunately, previous work in our laboratory on trimethylamine alane (TMAA) clearly suggests that a substitution reaction can occur when NH_2 is present.[27] With $(CH_3)_3NAlH_3$, the NH_2 is observed to replace the trimethylamine subunit thereby forming NH_2AlH_3 and $(CH_3)_3N$. With the current system, the analogous result would be

$$(CH_3)_3Al{:}NH_3 + NH_2 \rightarrow (CH_3)_3AlNH_2 + NH_3 \quad (2a)$$

or

$$(CH_3)_3Al{:}ND_3 + ND_2 \rightarrow (CH_3)_3AlND_2 + ND_3 \quad (2b)$$

in the case of ND_3 photolysis. We submit that eq 2 is a significant pathway for $(CH_3)_3AlNH_2$ formation. Of course, direct reaction of NH_2 with uncomplexed $(CH_3)_3Al$ via a three-body collision will also produce $(CH_3)_3AlNH_2$ and cannot be ruled out as a contributing mechanism.

2. Formation of Higher Mass Clusters. Although the formation of $(CH_3)_3Al{:}NH_2$ clearly arises from NH_3 photolysis to make NH_2, the higher order mass clusters (i.e., those that contain two or more Al atoms) do not. As an example, the laser power dependence as well as the ammonia pressure dependence for the $(CH_3)_3Al_2(NH_2)_2^+$ ion feature is much different from that for the $(CH_3)_3AlNH_2^+$ ion signal (see Figure 11). Such behavior is similar to that observed previously for GaN containing clusters.[14] These differences can be attributed to power-dependent competition among the single-photon dissociation,

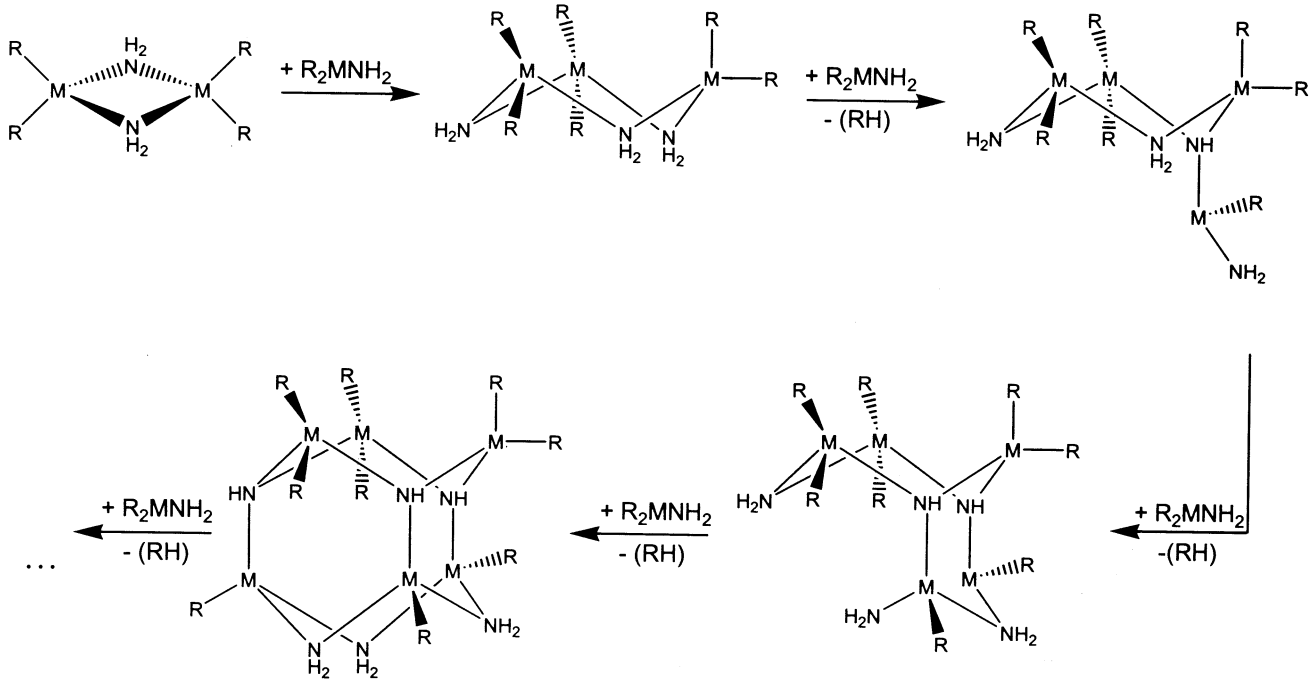

Figure 14. Schematic representation of $R_{2m+n}M_{m+n}(NH_2)_m(NH)_n$ cluster formation and structure where M is Al or Ga and R is CH_3.

multiphoton dissociation, and multiphoton ionization processes taking place during irradiation of a parent Al-containing compound (TMAl or TMAl:NH_3) and its associated photofragments. Note, too, that it is important to remember that the mass spectra on display contain EI-induced daughter fragments from the dissociation of parent ions and clusters in addition to the parent ions themselves, so equating observed ion signals with neutral species must be done with caution.

The $(CH_3)_3Al:NH_3$ adduct (as measured by the $(CH_3)_2Al:NH_3^+$ daughter fragment, mass 74) and the laser-induced clusters (represented by $(CH_3)_3Al_2(NH_2)_2^+$) display a similar dependence on NH_3 pressure. This similarity can be seen upon comparison of Figures 9 and 11a; i.e., both features saturate with increasing NH_3 pressure. Moreover, the large negative peaks for masses 74 and 77 shown in Figure 10b,c, respectively, clearly indicate that photolysis of the $(CH_3)_3Al:NH_3$ adduct is taking place. Such results suggest the presence of a direct photoinduced $(CH_3)_3Al:NH_3$ adduct clustering mechanism not unlike the thermal association process for GaN.[11,12] In contrast to the thermal process, however, our results at higher mass also reveal a propensity for creating clusters larger than trimers of $(CH_3)_2MNH_2$, specifically tetramers, pentamers, and hexamers. These results are shown in Figures 12 and 13 for both TMAl and TMGa in combination with NH_3.

Mechanistically, it has been proposed that the thermal growth of GaN via MOCVD occurs through a CH_4 elimination route involving $(CH_3)_3Ga:NH_3$ adducts.[12] In the case of the TMGa:NH_3 adduct, the energy required to eliminate methane is estimated to be ~2.1 eV.[8] It is known that elimination reactions are more facile for TMAl:NH_3 than the TMGa:NH_3 adduct.[28] This observation is directly related to the greater electropositive character of the Al over Ga, which correlates with the Al−N bond being stronger. Clearly, the 193 nm photon energy (6.4 eV) is enough to initiate the process. The resulting $(CH_3)_2GaNH_2$ radical intermediates can undergo polymerization reactions. In our case for $(CH_3)_3Al:NH_3$, the pathway would be

$$(CH_3)_3Al:NH_3 + h\nu\ (193\ nm) \rightarrow (CH_3)_3Al:NH_3)^* \rightarrow (CH_3)_2AlNH_2 + CH_4 \quad (3)$$

with subsequent radical polymerization

$$m(CH_3)_2AlNH_2 \rightarrow [(CH_3)_2AlNH_2]_m \quad (4)$$

expected for values of m at least up to 3. From Figures 12 and 13, it is clear that higher order ($m > 3$) clusters are being generated for both TMAl and TMGa. In fact, clusters containing at least six atoms of Al or Ga have been observed. Calculations with subsequent discussion by Timoshkin et al. in the case of TMGa and NH_3 predict the existence of such species due to highly favorable energetics.[15] A possible pathway for such growth is depicted in Figure 14.

Though not conclusive, our results are consistent with the CH_4 elimination pathway provided in Figure 14. Once a trimeric species is generated, the hexamer could be generated by either dimerization of the trimer or continued monomeric addition to the trimer. The data suggest the latter owing to the observation of four and five membered cluster units. However, note that their existence may be due to the presence of the neutral clusters themselves or perhaps to daughter fragments from the ionization/fragmentation of a six-membered species. Consequently, we cannot rule out the dimerization channel as the route for hexamer formation.

Acknowledgment. Financial support from the Department of Energy, the State of Louisiana via the Louisiana Education Quality Support Fund, NASA, and the National Science Foundation through Tulane University's Center for Photoinduced Processes is very much appreciated. An equipment donation from AT&T/Lucent is also gratefully noted.

References and Notes

(1) Ponce, F. A., Moustakas, T. D., Akasaki, I., Monemar, B. A., Eds. *III−V Nitrides*; Materials Research Society Symposium Proceedings 449; Materials Research Society: Pittsburgh, PA, 1997.
(2) Abernathy, C. R., Amano, H., Zopler, J. C., Eds. *Gallium Nitride and Related Materials II*; Materials Research Society Symposium Proceedings 468; Materials Research Society: Pittsburgh, PA, 1997.
(3) Riechert, H.; Averbeck, R.; Graber, A.; Schienle, M.; Strauss, U.; Tews, H. *Mater. Res. Soc. Symp. Proc.* **1997**, *449*, 149.
(4) Donnelly, V. M.; Brasen, D.; Appelbaum, A.; Geva, M. *J. Appl. Phys.* **1985**, *58*, 2022.
(5) Aoyagi, Y.; Masuda, S.; Namba, S. *Appl. Phys. Lett.* **1986**, *49*, 880.
(6) Zinck, J. J.; Brewer, P. D.; Jensen, J. E.; Olson, G. L.; Tutt, L. W. *Mater. Res. Soc. Symp. Proc.* **1987**, *75*, 233.
(7) Demchuk, A.; Cahill, J. J.; Koplitz, B. *Chem. Mater.* **2000**, *12*, 3192.
(8) Coates, G. E. *J. Chem. Soc.* **1951**, 2003.
(9) Zaouk, A.; Salvetat, E.; Sakaya, J.; Maury, F.; Constant, G. *J. Cryst. Growth* **1981**, *55*, 135.
(10) Moss, R. H. *J. Cryst. Growth* **1984**, *68*, 78.
(11) Almond, M. J.; Drew, M. G. B.; Jenkins, C. E.; Rice, D. A. *J. Chem. Soc., Dalton Trans.* **1992**, *1*, 5.
(12) Thon, A.; Kuech, T. F. *Appl. Phys. Lett.* **1996**, *69*, 55.
(13) Demchuk, A.; Porter, J.; Beuscher, A.; Dilkey, A.; Koplitz, B. *Chem. Phys. Lett.* **1998**, *283*, 231.
(14) Demchuk, A.; Porter, J.; Koplitz, B. *J. Phys. Chem. A* **1998**, *102*, 8841.
(15) Timoshkin, A. Y.; Bettinger, H. F.; Schaefer, H. F. *J. Phys. Chem. A* **2001**, *105*, 3249.
(16) Henrickson, C. H.; Eyman, D. P. *Inorg. Chem.* **1967**, *6*, 1461.
(17) Brum, J. L.; Tong, P.; Koplitz, B. *Appl. Phys. Lett.* **1990**, *56*, 695.
(18) Mitchell, S. A.; Hackett, P. A. *J. Chem. Phys.* **1983**, *79*, 4815.
(19) Mitchell, S. A.; Hackett, P. A.; Rayner, D. M.; Humphries, M. R. *J. Chem. Phys.* **1985**, *83*, 5028.
(20) McGrary, V. R.; Donelley, V. M. *J. Cryst. Growth* **1987**, *84*, 253.
(21) Beuermann, Th.; Stuke, M. *Appl. Phys. B* **1989**, *49*, 145.
(22) Zhang, Y.; Beuermann, Th.; Stuke, M. *Appl. Phys. B* **1989**, *48*, 97.
(23) Demchuk A.; Porter J.; Koplitz B. *Fundamental Gas-Phase and Surface Chemistry of Vapor-Phase Materials Synthesis;* Allendorf, M. D., Zachariah, M. R., Mountziaris, L., McDaniel, A. H., Eds.; *ECS Proceedings*; The Electrochemical Society, Inc.: Pennington, NJ, 1999; No. 98−23, p 129.
(24) Thayer, J. S. *Organometallic Chemistry*; VCH Publisher: New York, 1988; pp 31−38.
(25) Okabe, H. *Photochemistry of Small Molecules*; Wiley-Interscience: New York, 1978; pp 269−272.
(26) Donnelly, V. M.; Baronavski, A. P.; McDonald, J. R. *Chem. Phys.* **1979**, *43*, 271.
(27) Demchuk, A.; Cahill, J. J.; Simpson, S.; Koplitz, B. *Chem. Phys. Lett.* **2001**, *348*, 217.
(28) Waggoner, K. M.; Power, P. P. *J. Am. Chem. Soc.* **1991**, *113*, 3385.